Proceedings of the ASME 2018 Dynamic Systems and Control Conference
DSCC 2018
September 30-October 3, 2018, Atlanta, Georgia, USA

DSCC2018-9208

CHARACTERIZING COMBUSTION INSTABILITY USING DEEP CONVOLUTIONAL NEURAL NETWORK

Tryambak Gangopadhyay*, Anthony Locurto, Paige Boor, James B. Michael, Soumik Sarkar
Department of Mechanical Engineering
Iowa State University
Ames, Iowa 50011
Email: {tryambak, alocurto, pkboor, jmichael, soumiks}@iastate.edu

ABSTRACT

Detecting the transition to an impending instability is important to initiate effective control in a combustion system. As one of the early applications of characterizing thermoacoustic instability using Deep Neural Networks, we train our proposed deep convolutional neural network (CNN) model on sequential image frames extracted from hi-speed flame videos by inducing instability in the system following a particular protocol- varying the acoustic length. We leverage the sound pressure data to define a non-dimensional instability measure used for applying an inexpensive but noisy labeling technique to train our supervised 2D CNN model. We attempt to detect the onset of instability in a transient dataset where instability is induced by a different protocol. With the continuous variation of the control parameter, we can successfully detect the critical transition to a state of high combustion instability demonstrating the robustness of our proposed detection framework, which is independent of the combustion inducing protocol.

I. INTRODUCTION

Many early warning measures have been developed over the years to detect the onset of critical transitions in dynamical systems. Early detection of critical transitions can help in developing adequate strategies to prevent unwanted events. Although we are far from being able to develop accurate models to predict critical threshold, early warning signals may be a significant step to judge whether the probability of such an event is increasing for complex dynamical systems ranging from ecosystems to financial markets and climate which may show a sudden shift to a contrasting dynamical regime [1]. Critical transitions can occur in turbulent combustors which are widely used in propulsion and power systems. These transitions can have many adverse effects on the performance of combustion dependent power generating systems resulting in enormous revenue loss.

The unsteady flow perturbations resulting in heat release rate fluctuations in a combustor makes it susceptible to thermoacoustic instabilities characterized by large amplitude pressure oscillations with sharp tones. The oscillations arising as a result of nonlinear coupling between the flame and the acoustic field can cause an intense growth of pressure fluctuations and increased heat transfer on the combustor surfaces [2–4]. These oscillations can result in structural damage and catastrophic failures of the engine [5]. The positive feedback mechanism established between the sound waves and heat release rate gives rise to this transition to large amplitude oscillations. Characterizing combustion instability is therefore important for early detection of this transition which can lead to effective control and performance monitoring of the engines.

In order to characterize combustion instabilities, full-scale computational-fluid-dynamic (CFD) models and/or reduced-order models have been developed, but these models may have imperfect validation due to several restrictions which include simplifying assumptions, inherent complexities, and computational restrictions. Many researchers have conducted studies on physics-based modeling of instabilities (e.g., [6–8]). Coherent structures are fluid mechanical phenomena associated with the

*Address all correspondence to this author.

coherent phase of vorticity and having high levels of vorticity among others [9] which can cause large-scale velocity oscillations and overall flame shape oscillations by curling and stretch. The commonly used methods for detection of coherent structures are proper orthogonal decomposition (POD) [10] and dynamic mode decomposition (DMD) [11]. The abundant presence of coherent structure indicates instability [12] but lack of physical understanding of these structures makes it difficult to identify the precursors of instability.

Researchers have also explored precise control of fuel flow in order to suppress or avoid thermo-acoustic instabilities [13, 14]. An alternative is to use dynamic data-driven application systems [15] based on time series data of physical sensors and images to identify the features that can characterize combustion instabilities (e.g., [16–19]). Gotoda et al. [20] investigated the dynamic behavior of the combustion instability using non-linear time series analysis in combination with a surrogate data method.

With recent advancements in deep learning, neural network approaches can effectively extract features from raw data for automated learning and discriminative tasks and deep learning is found to be apparently superior to other state-of-the-art machine learning tools for handling very large-dimensional data spaces and learning features [21]. A deep convolutional neural network (CNN) can learn meaningful patterns from images [22]. The concepts of deep learning have been used in the domains of image, video and speech processing extensively. Farabet et al. [23] used a multiscale convolutional network to extract features for scene labeling. Others applications based on convolutional neural network include gradient-based learning applied to handwritten digit recognition task [24], multitask learning for natural language processing [25], natural low-light image enhancement [26]. Applications of deep learning in studying combustion instability have been very limited. Sarkar et al. [27] applied a deep learning-based framework to extract features from hi-speed flame images for early detection of combustion instability. A neural-symbolic framework can be used to first extract low-dimensional features from sequential hi-speed flame images using a deep convolutional neural network (CNN) and then the temporal variation can be captured using Symbolic Time Series Analysis (STSA) [28]. Akintayo et al. [29] designed an end-to-end convolutional selective autoencoder which encodes the coherent structure information from the unstable frames. 3D CNN architecture can be applied to leverage the temporal correlations among the consecutive frames and classify flame images into two classes- stable and unstable [30].

Extracting features from a large volume of sequential hi-speed frames for conditions falling in the regime of instability is essential for characterizing combustion instability. Developing a robust instability detection framework is crucial for applying effective control strategies to mitigate the probabilities of occurrence of such events at an early stage. However, the previous works are mostly concentrated on testing the model for detecting the onset of instability induced by the same mechanism as that for the training set. In this paper, we propose for the first time an image-based detection framework which is independent of the combustion inducing protocol. Also, we leverage both the sound pressure data and hi-speed images to train our model. We induce instability in the system by varying the acoustic length and use the sequential image frames extracted from hi-speed flame videos to train our 2D CNN model. For training our supervised model, the labels are generated with an inexpensive but noisy labeling technique using a moving window approach on the sound pressure time series data. To demonstrate the robustness of the framework, we attempt to detect the critical transition where the combustion instability is induced by a different protocol. We use equivalence ratio as the control parameter keeping the acoustic length fixed. With the continuous variation of the control parameter, the framework successfully detects the impending transition and we define a non-dimensional expected instability measure which aids in estimating the extent of instability pertaining to a particular condition. This may be a significant step towards accurate detection of the onset of transition which can eliminate adverse effects on the performance of combustion systems.

II. EXPERIMENTAL SETUP, DATASET COLLECTION AND PRE-PROCESSING

This section presents a brief description of the experimental setup followed by the details of dataset collection and data preprocessing.

Experimental Setup

A Rijke tube having two open ends and a heat source shows instability when the heat source is in a certain region within the upstream half of the tube and with an unsteady transfer of energy from the heat source to the air [31]. To depict an acoustically coupled instability, we use a vertically placed open-ended Rijke tube setup with the mean flow of a premixed fuel as shown in Fig. 1. The Pyrex glass tube is 24 inches long with a diameter of 3 inches. The burner is a stainless steel tube of diameter 0.375 inches placed concentric to the Pyrex tube. We use a conical steel bluff body (inner diameter= 7 mm, outer diameter= 9.525 mm) with an approximate distance of 10.38 mm measured from the burner to the tip of the bluff body. Air at ambient temperature, used as the oxidizer and ethylene are premixed at stoichiometric conditions. The flow rates of the fuel and air are controlled using Alicat M-Series flow controllers. A Photron Fastcam is used for capturing hi-speed flame images and a Sony microphone connected to a Tektronix oscilloscope records the acoustic signal.

Data Collection

In the present work, we vary the position of the burner tip with respect to the ends of the Rijke tube by changing the x/L

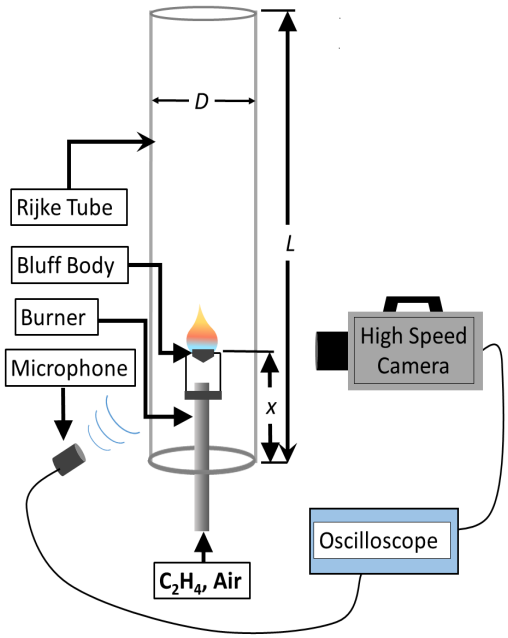

FIGURE 1. SCHEMATIC OF THE EXPERIMENTAL SETUP.

ratio (Fig. 1) from 0.125 to 0.5 keeping the air and fuel flow rates constant at 18 SLPM and 1.5 SLPM respectively. We pose our characterizing problem based on the data collected at five different flame positions.

The hi-speed camera (Photron FASTCAM SA5 1000K-M2) captures 5000 frames per second with an exposure of 1/5000 seconds and resolution of 192 x 352 pixels^2. The microphone placed in the field of sound (approximately 12 inches from the tube) starts recording after triggering of the oscilloscope with the Photron camera. The oscilloscope (Tektronix MSO 70404C) has a sampling rate of 5 MS/s and total record length of 100 Million data points. The three channels of the oscilloscope record the trigger signal from the camera, microphone signal and the camera frame rate respectively.

For each location after igniting the flame, we wait 10 seconds to trigger the oscilloscope. Datasets are captured non-sequentially with x/L. We start the experiment at burner location(x) 3" instead of starting at location 0". We then move to location 12" for recording the next dataset followed by locations 6", 0" and 9" as shown in Table 1.

Due to the limitation of the camera memory, we can store 33.88 secs of video data at a time. At a particular burner location, we use two partitions to capture images each with a time length of 16.94 secs. Thus we record two separate datasets (each having 84700 images) corresponding to every location. We simultaneously record the acoustic pressure signal and capture the

TABLE 1. THE DIFFERENT BURNER LOCATIONS.

Burner Location (in inches)	x/L
3	0.125
12	0.5
6	0.25
0	0
9	0.375

hi-speed flame images so that the two datasets can be correlated. The data recorded at 5 different burner locations is used for training the 2D CNN model.

We perform the experiment at the burner location 6" by continuously varying the control parameter to record the transient data for capturing the transition to a state of high combustion instability. Keeping the fuel flow rate constant at 1.5 SLPM, we increase air flow rate every 4 secs by 2 SLPM starting from 16 SLPM and ending at 22 SLPM. Therefore, the control parameter is the equivalence ratio which is decreased gradually from 1.5 to 0.95 by increasing the air flow rate. We use this dataset for testing to show the robustness of our image-based detection framework.

Data Preprocessing

For each burner location, we have a total record length of 33.88 secs for two partitions each with a record length of 16.94 secs. The resolution of the flame chemiluminescence images extracted from the hi-speed video is 192 x 352 as shown in Fig. 2. We crop the images to remove most of the dark background portion and concentrate on the flame. Each cropped image has a resolution of 160 x 130. The cropped images are then resized to dimensions of 128 x 128 to be used as input to our 2D CNN model.

A moving window approach has been used previously to investigate the dynamic characteristics of a combustion system [18]. We utilize a moving window approach by splitting the entire sound pressure time series recorded at each burner location into consecutive windows of length 0.1s (100 ms) each and analyze the windows sequentially one-by-one as shown in Fig. 3. For each window power spectral density plot is computed and each 0.1s window corresponds to 500 images with the hi-speed camera fps at 5000. At a particular location, we consider 16 secs time series data at the beginning of each partition from a total record length of 16.94 secs and thus yielding 320-time windows for both partitions. In total for five locations, we have 1600 time windows and we compute FFT plots for all the time windows separately.

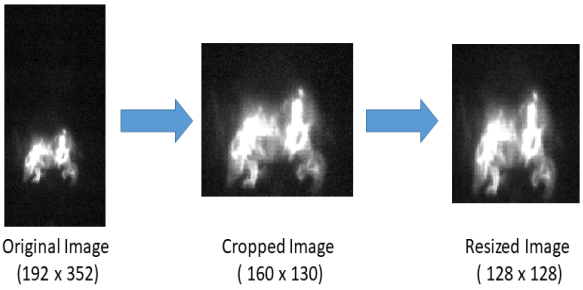

FIGURE 2. PRE-PROCESSING OF A SAMPLE FLAME IMAGE CAPTURED AT x/L=0.125. THE IMAGES ARE CROPPED TO REMOVE MOST OF THE DARK BACKGROUND PORTION AND THE CROPPED IMAGES ARE RESIZED.

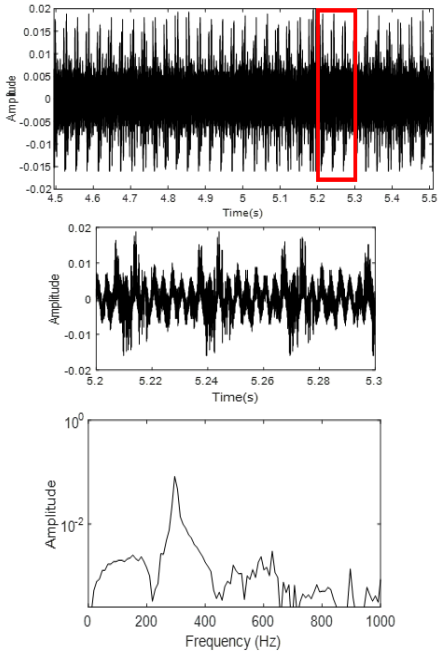

FIGURE 3. MOVING WINDOW APPROACH - SELECTING A WINDOW OF 0.1 SECS FROM PRESSURE TIME SERIES AND THE CORRESPONDING POWER SPECTRAL DENSITY PLOT AT x/L=0.125.

III. PROBLEM FORMULATION AND METHOD USED

In this section, we state our problem formulation by defining instability measure and thereafter applying Maximum Entropy Partitioning to generate the labels. We also describe our proposed 2D CNN model used for classification.

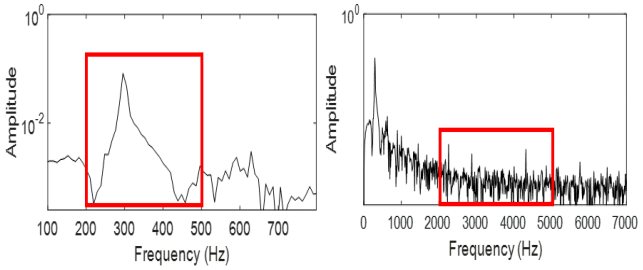

FIGURE 4. TWO DIFFERENT FREQUENCY RANGES (200 - 500) AND (2000 - 5000) HIGHLIGHTED IN THE FIGURE - USED TO COMPUTE INSTABILITY MEASURE.

Instability Measure and Labeling using Maximum Entropy Partitioning

From the FFT plot, we choose a frequency range 2000-5000 Hz and calculate the mean of all corresponding amplitudes falling in that range. This gives us an estimate of the amplitude of the noise in the system. The frequency range (2000-5000 Hz) is chosen as it is far away from the range where the dominating frequencies exist, thus giving an estimate of the noise. We observe that the dominating frequencies with very high corresponding amplitudes generally fall in the frequency range 200-500 Hz for all the 1600 time windows. We select this frequency range (200- 500 Hz) and add all the amplitudes in this range to get an idea of the overall energy content of the instability existing in the system. We illustrate the two chosen frequency ranges in Fig. 4.

$$IM = \frac{\sum \text{Amplitudes in the range 200-500 Hz}}{\text{Mean of the amplitudes in the range 2000-5000 Hz}} \quad (1)$$

We define the Instability Measure (IM) in Eqn. (1). The scatter plot of instability measure values for all the 1600 time windows is shown in Fig. 5. We observe that the values of IM vary from 183.79 to 3959.30 and thus comprise a large range of values illustrating low to high instability. We partition the IM values into 5 partitions using the maximum entropy principle [32]. Each discretized partition comprises of 320-time windows corresponding to data of length 32 secs. We correlate the captured hi-speed flame images with the time windows and therefore we aggregate 160,000 images per partition. The classes are defined based on the range of IM values as illustrated in Table 2. The label for a particular image is generated based on the IM of the corresponding time window it belongs to. We use this dataset as input for training our image-based 2D CNN model where a higher value of label indicates higher instability. With a total of 800,000 images, maximum entropy partitioning ensures we have an equal

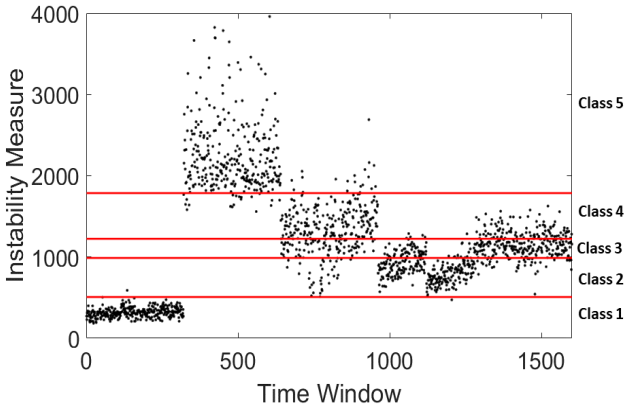

FIGURE 5. VALUES OF INSTABILITY MEASURE FOR ALL TIME WINDOWS AND SHOWING 5 PARTITIONS COMPUTED FROM MAXIMUM ENTROPY PARTIONING.

TABLE 2. VALUES OF INSTABILITY MEASURES FOR FIVE CLASSES .

Instability Measure Range	Class
(183.79 - 507.49)	1
(507.49 - 988.24)	2
(988.24 - 1223.80)	3
(1223.80 - 1786.60)	4
(1786.60 - 3959.30)	5

number of images (160,000) per class. This labeling technique is inexpensive as it does not involve manual labeling of all the images and also consumes less time. The technique can be interpreted noisy as it involves aggregation of images in a particular class from images corresponding to different burner locations. But it helps in further generalizing our problem formulation as we don't restrict ourselves to the dynamic characteristics of a particular experimental condition for labeling.

Method

2D Convolutional Neural Network. In an image, partial edges and corners are low-level features and the combination of edges and corners are high-level features. With the focus on learning features from the data, deep learning is an emerging branch of machine learning being used nowadays for a wide range of applications. The field of computer vision is advancing rapidly with developments in deep learning. Deep learning computer vision finds many applications including self-driving cars, face recognition, etc. Rapid advancement in computer vision is now enabling new applications that were not possible earlier.

Convolutional neural networks(CNN) are discriminative models which use nonlinear mapping to perform dimension reduction of data primarily from the local neighborhood. Compared to fully connected layers, convolutional (conv.) networks have fewer trainable parameters as there exists shared weights in each unit of the feature maps. Conv. nets are specifically designed to deal with the variability of 2D shapes and can outperform all other techniques for an image recognition task like handwritten digit recognition [24]. Shared weights and subsampling result in the invariance property of convolutional nets [33].

In a traditional feedforward neural network, the flattening of the image to a one-dimensional vector results in loss of all spatial structure in the image. Traditional networks are also hard to train when the images are not perfectly resized. For large images, the number of parameters in fully connected networks become very large and that makes it difficult to get enough data to prevent the neural network from overfitting. Also, the computational and memory requirements increase multifariously. To use large images, the convolution operation is used which is one of the fundamental building blocks in a CNN. Conv. nets preserve the spatial relationship between pixels by learning features across the whole image. The kernels(filters) in a CNN are the neurons of the layer having input weights. In the first layer, the input values are the pixel values of the image. Deeper in the network architecture, the convolutional layer takes input from a feature map of the previous layer.

Following a sequence of one or more conv. layers, pooling layer is used to down-sample the feature map from the previous layers. Pooling layers compress the feature representations and reduce the overfitting of the training data by the model. Pooling layers speed up computation as well and make some features more robust. We use max-pooling layers in our model which take the maximum of the input value to create its own feature map. Max Pooling has a set of hyperparameters (filter size and stride) but no parameters to learn. After the convolutional and pooling layers extract the features, fully connected layers are used at the end to generate non-linear combinations of the features and finally to predict the classes. Fully connected layers generally have a non-linear activation function or a softmax activation to output the class prediction probabilities.

We propose a Convolutional Neural Network framework to classify flame chemiluminescence images into 5 classes. The network architecture is illustrated in Fig. 6. Our proposed CNN architecture is different from the ones used by previous researchers [22, 34]. We use fixed-sized 128 x 128 grayscale images as input to our supervised model. A conv. layer is used following the first convolutional layer. Both layers have 32 filters each and a receptive field of width 7 pixels and height 7

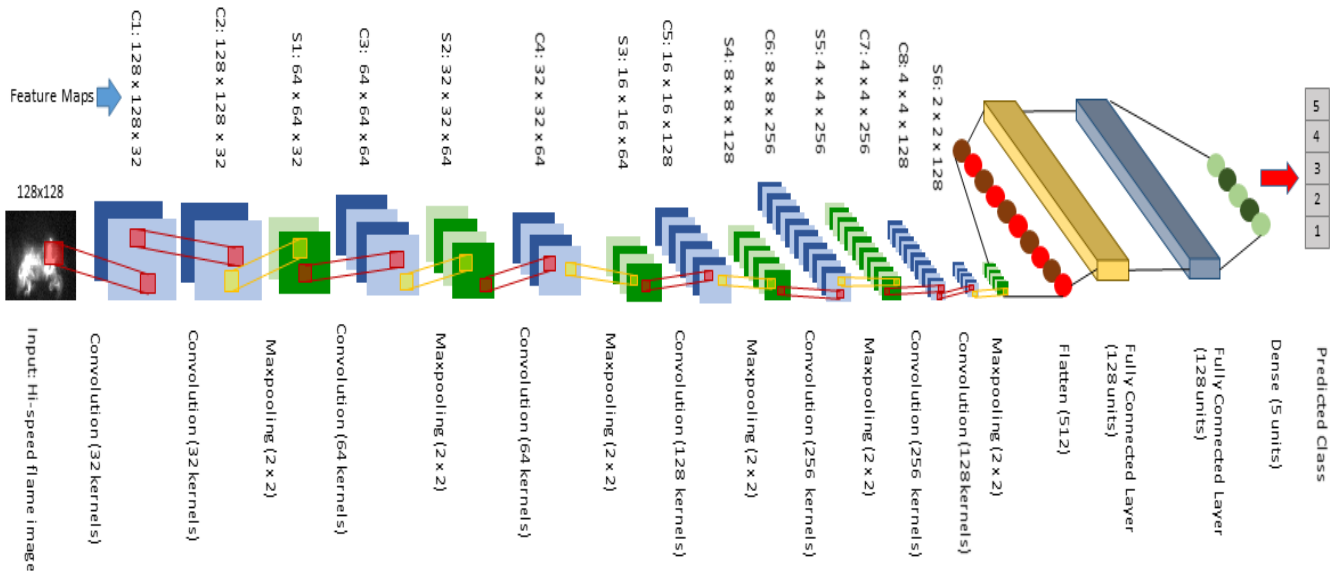

FIGURE 6. PROPOSED DEEP CONVOLUTION NEURAL NETWORK ARCHITECTURE

pixels. Instead of using small receptive fields throughout the network [34], we start with 7 x 7 receptive fields for first two conv. layers and for the next two conv. layers we use 5 x 5 receptive fields. The conv. layers deeper in the network have 3 x 3 receptive fields. Our configuration is less deep than VGG-16 [34], though it is deeper than AlexNet [22]. We increase the number of filters from 32 for the first two conv. layers to 256 in the deeper layers.

Six max-pooling layers are used, but not all the conv. layers are followed by max-pooling as shown in Fig. 6. All max-pooling layers have a 2 x2 receptive field and a stride of 2 to avoid any overlap. The resulting feature maps from a max-pooling layer are one half the size of the input feature maps. The fully-connected (FC) layers are used after the stack of convolutional and max-pooling layers. The first two FC layers have 128 channels each and the third layer contains 5 channels for 5- class classification. We use softmax as the final layer. Rectified Linear Unit (ReLU) non-linearity [22] is used for all the conv. layers and we perform Batch Normalization [35] at each layer.

To prevent overfitting, we use dropout regularization method [36] where neurons need to learn more robust features rather than relying on the presence of, particularly other neurons. We use dropout regularization after the max-pooling layers, flatten layer and the first two FC layers. We gradually increase the dropout regularization probability from 0.1 in the first layers to 0.5 in the FC layers. This helps in avoiding much loss of information in the first layers. With the use of dropout, we require an additional number of epochs to converge. The total number of trainable parameters for this model is about 1.54 million (1,544,933) while there are 2,432 non-trainable parameters. The framework is performed on NVIDIA GPUs and implemented using Keras [37] with the TensorFlow backend [38].

IV. RESULTS AND DISCUSSIONS

We use categorical cross-entropy as the loss function for our experiments. Adam optimization technique [39] is used with all the default parameters (learning rate of 0.001) and we train our model with a batch size of 128 samples. To decrease the training time, we randomly select 264,000 images out of 800,000 images and then split it into training and test sets: 250,800 training examples and 13200 test examples. Therefore we have 50,160 training images for each class. The validation set is used as the test set for the experiments.

The accuracy plot is illustrated in Fig. 7. We achieve the training set accuracy of 98.04% which can improve after training for more epochs as evident from its slowly converging nature. The validation/test set accuracy is 83.02% with our proposed 2D CNN model. The class-wise accuracies on validation set are tabulated in Table 3. For Class 1, our model achieves 100% accuracy while for Class 5 it shows 96% accuracy. It indicates that the model can predict the two extreme conditions of instability measures (Class 1 and Class 5) with high accuracy.

The performance of a classification algorithm can be examined using a confusion matrix. Here, element (i,j) gives a measure of the empirical probability of predicting class j when the

TABLE 3. PERFORMANCE ON VALIDATION/TEST SET.

Class	Accuracy
1	100%
2	81%
3	69%
4	69%
5	96%

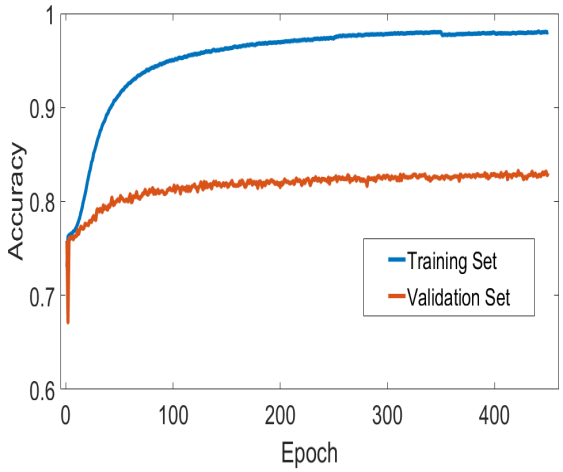

FIGURE 7. ACCURACY PLOT FOR TRAINING AND VALIDATION/TEST SET AFTER 450 EPOCHS

true label is i.The diagonal elements represent the number of points for which the predicted label is equal to the true label thus indicating correct predictions, while off-diagonal elements are those that are mislabeled by the classifier [40]. The normalized confusion matrix is shown in Fig. 8. When the true Class is 4, the 2D CNN model confuses mainly with Class 3 as observed in row 4. The confusion between true Class 3 with Class 2 and Class 4 is manifested in row 3 of the confusion matrix. The model has an accuracy of 81% while predicting Class 2 with the mislabeling occurring mostly with Class 3. Thus the errors of our model for Classes 2, 3 and 4 mainly come from mislabeling with the nearest classes and it signifies that our model can predict the classes with intermediate values of instability measures fairly well.

$$E = \frac{\sum_{class=1}^{5}(IM)_{class}(\text{No. of predictions})_{class}}{\sum_{class=1}(\text{No. of predictions})_{class}} \qquad (2)$$

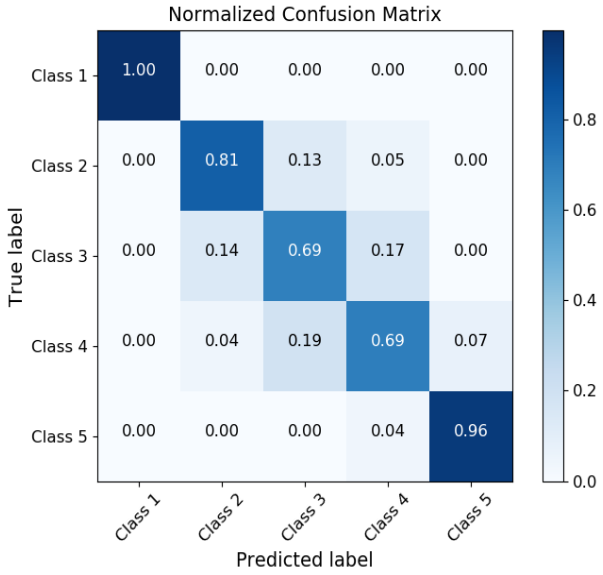

FIGURE 8. CONFUSION MATRIX SHOWING PERFORMANCE ON VALIDATION/TEST SET

We define the Expected Instability Measure (E) in Eqn. (2) to search for forewarning signals of the critical transition to a state of high combustion instability. The $(IM)_{class}$ value is the mean of the instability measures for all training samples corresponding to each class as shown in Table 2. The values of $(IM)_{class}$ for five classes are 345.64, 747.87, 1106, 1505.20 and 2872.90 respectively. To test the performance of our model on a transient dataset, we study the change in the values of E by varying the control parameter continuously. The trained model is used for prediction on the hi-speed images captured at the conditions corresponding to each value of the control parameter. The results comprise the number of predictions for each class which is leveraged to calculate the value of expected instability measure (E) at that particular condition as defined in Eqn. (2).

Keeping the fuel flow rate constant and increasing the air flow rate, our control parameter is the equivalence ratio which is decreased gradually from 1.5 to 0.95 as shown in Fig. 9. The value of E is reasonably low when we start our experiment at equivalence ratio 1.31 indicating less chance of the presence of instability. We observe a large increase in the value of E when the equivalence ratio is decreased to 1.17. This significant increase in the expected instability measure indicates the possibility of critical transition to a state of higher expected combustion instability and may help in robust detection of the impending condition of maximum combustion instability observed with a further decrease of the equivalence ratio to 1.05. Going more towards the leaner side from the condition of maximum instability, the value of E decreases demonstrating a decrease in the extent of

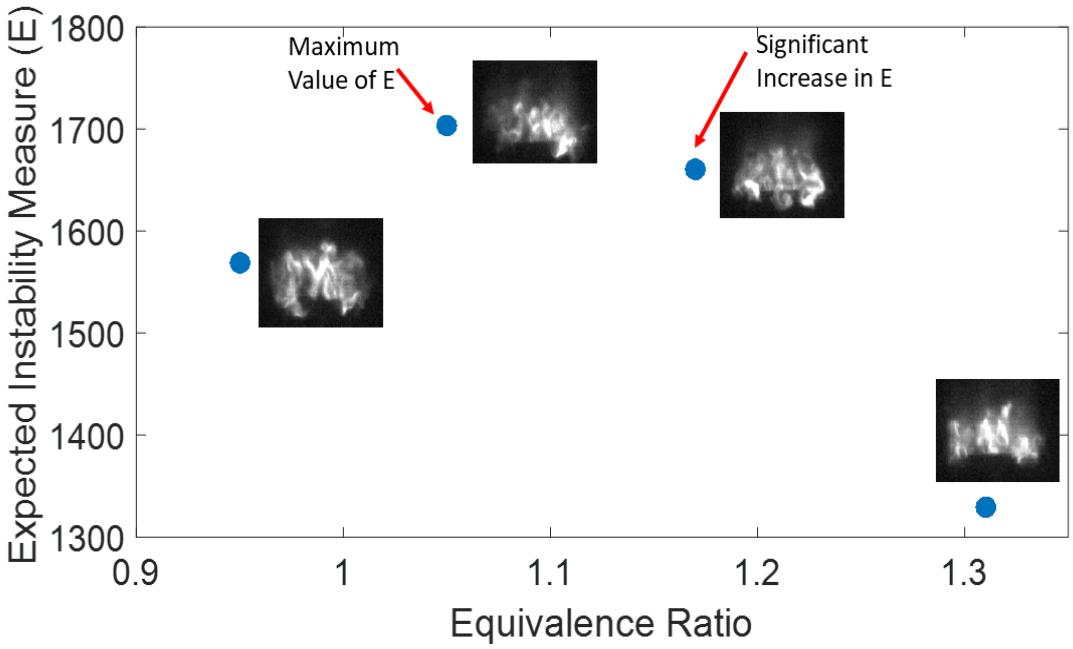

FIGURE 9. VARIATION OF EXPECTED INSTABILITY MEASURE (E) WITH EQUIVALENCE RATIO

the existing instability of the system.

V. SUMMARY, CONCLUSIONS AND FUTURE WORK

In this paper, we propose an image-based detection framework using deep convolutional neural networks to characterize combustion instability. The robust framework, independent of the combustion inducing protocol may be a significant step towards accurately detecting the onset of transition to an impending instability.

We induce an instability in the system by varying the acoustic length and leverage the sound pressure time series data to define a non-dimensional instability measure. We apply an inexpensive but noisy labeling technique on the values of this measure using Maximum Entropy Partitioning, to generate labels for hi-speed flame images to train our supervised 2D CNN model. We use a different combustion inducing protocol to test our model and we define a non-dimensional expected instability measure to estimate the extent of instability existing at a particular condition. We continuously vary equivalence ratio as the control parameter and capture sequential hi-speed flame images to detect the critical transition. The framework demonstrates robustness by successfully detecting the sudden transition to a state of higher combustion instability.

Robust detection of the critical transition can help in initiating effective control actions in a combustion system as it approaches a state of instability. The expected instability measure value may indicate whether the probability of occurrence of such an impending instability is increasing and early warning signals are crucial for mitigation of such events to avoid the adverse effects on the performance of combustion systems.

One of the immediate next steps is to achieve a higher validation accuracy. The future work will involve the incorporation of temporal knowledge in the model to improve the detection framework further and this can be achieved using Convolutional LSTM and 3D CNN architectures which are designed for sequence prediction problems with spatial inputs.

ACKNOWLEDGMENT

This work has been supported in part by the U.S. Air Force Office of Scientific Research under the YIP grant FA9550-17-1-0220. Any opinions, findings and conclusions or recommendations expressed in this publication are those of the authors and do not necessarily reflect the views of the sponsoring agency.

REFERENCES

[1] Scheffer, M., Bascompte, J., Brock, W. A., Brovkin, V., Carpenter, S. R., Dakos, V., Held, H., Van Nes, E. H., Rietkerk, M., and Sugihara, G., 2009. "Early-warning signals for critical transitions". *Nature,* ***461***(7260), p. 53.

[2] Rayleigh, J. W. S., 1878. "The explanation of certain acoustical phenomena". *Nature,* ***18***(455), pp. 319–321.

[3] Dowling, A. P., 1997. "Nonlinear self-excited oscillations of a ducted flame". *Journal of fluid mechanics,* ***346***, pp. 271–290.

[4] Culick, F., and Kuentzmann, P., 2006. Unsteady motions in combustion chambers for propulsion systems. Tech. rep., NATO RESEARCH AND TECHNOLOGY ORGANIZATION NEUILLY-SUR-SEINE (FRANCE).

[5] Fisher, S. C., and Rahman, S. A., 2009. "Remembering the giants: Apollo rocket propulsion development".

[6] Palies, P., Schuller, T., Durox, D., and Candel, S., 2011. "Modeling of premixed swirling flames transfer functions". *Proceedings of the combustion institute,* ***33***(2), pp. 2967–2974.

[7] Bellows, B. D., Bobba, M. K., Forte, A., Seitzman, J. M., and Lieuwen, T., 2007. "Flame transfer function saturation mechanisms in a swirl-stabilized combustor". *Proceedings of the combustion institute,* ***31***(2), pp. 3181–3188.

[8] Noiray, N., Durox, D., Schuller, T., and Candel, S., 2008. "A unified framework for nonlinear combustion instability analysis based on the flame describing function". *Journal of Fluid Mechanics,* ***615***, pp. 139–167.

[9] Hussain, A. K. M. F., 1983. "Coherent structures - Reality and myth". *Physics of Fluids,* ***26***, Oct., pp. 2816–2850.

[10] Berkooz, G., Holmes, P., and Lumley, J. L., 1993. "The proper orthogonal decomposition in the analysis of turbulent flows". *Annual review of fluid mechanics,* ***25***(1), pp. 539–575.

[11] Schmid, P. J., 2010. "Dynamic mode decomposition of numerical and experimental data". *Journal of fluid mechanics,* ***656***, pp. 5–28.

[12] Chakravarthy, S. R., Shreenivasan, O. J., Boehm, B., Dreizler, A., and Janicka, J., 2007. "Experimental characterization of onset of acoustic instability in a nonpremixed half-dump combustor". *The Journal of the Acoustical Society of America,* ***122***(1), pp. 120–127.

[13] Gorinevsky, D., Overman, N., and Goeke, J., 2012. "Amplitude and phase control in active suppression of combustion instability". In American Control Conference (ACC), 2012, IEEE, pp. 2601–2608.

[14] Banaszuk, A., Ariyur, K. B., Krstić, M., and Jacobson, C. A., 2004. "An adaptive algorithm for control of combustion instability". *Automatica,* ***40***(11), pp. 1965–1972.

[15] Darema, F., 2005. "Dynamic data driven applications systems: New capabilities for application simulations and measurements". In International conference on computational science, Springer, pp. 610–615.

[16] Nair, V., and Sujith, R., 2014. "Multifractality in combustion noise: predicting an impending combustion instability". *Journal of Fluid Mechanics,* ***747***, pp. 635–655.

[17] Nair, V., Thampi, G., Karuppusamy, S., Gopalan, S., and Sujith, R., 2013. "Loss of chaos in combustion noise as a precursor of impending combustion instability". *International journal of spray and combustion dynamics,* ***5***(4), pp. 273–290.

[18] Sen, U., Gangopadhyay, T., Bhattacharya, C., Mukhopadhyay, A., and Sen, S., 2018. "Dynamic characterization of a ducted inverse diffusion flame using recurrence analysis". *Combustion Science and Technology,* ***190***(1), pp. 32–56.

[19] Ghosal, S., Ramanan, V., Sarkar, S., Chakravarthy, S. R., and Sarkar, S., 2016. "Detection and analysis of combustion instability from hi-speed flame images using dynamic mode decomposition". In ASME 2016 Dynamic Systems and Control Conference, American Society of Mechanical Engineers, pp. V001T12A005–V001T12A005.

[20] Gotoda, H., Nikimoto, H., Miyano, T., and Tachibana, S., 2011. "Dynamic properties of combustion instability in a lean premixed gas-turbine combustor". *Chaos: An Interdisciplinary Journal of Nonlinear Science,* ***21***(1), p. 013124.

[21] Hinton, G. E., and Salakhutdinov, R. R., 2006. "Reducing the dimensionality of data with neural networks". *science,* ***313***(5786), pp. 504–507.

[22] Krizhevsky, A., Sutskever, I., and Hinton, G. E., 2012. "Imagenet classification with deep convolutional neural networks". In Advances in neural information processing systems, pp. 1097–1105.

[23] Farabet, C., Couprie, C., Najman, L., and LeCun, Y., 2013. "Learning hierarchical features for scene labeling". *IEEE transactions on pattern analysis and machine intelligence,* ***35***(8), pp. 1915–1929.

[24] LeCun, Y., Bottou, L., Bengio, Y., and Haffner, P., 1998. "Gradient-based learning applied to document recognition". *Proceedings of the IEEE,* ***86***(11), pp. 2278–2324.

[25] Collobert, R., and Weston, J., 2008. "A unified architecture for natural language processing: Deep neural networks with multitask learning". In Proceedings of the 25th international conference on Machine learning, ACM, pp. 160–167.

[26] Lore, K. G., Akintayo, A., and Sarkar, S., 2017. "Llnet: A deep autoencoder approach to natural low-light image enhancement". *Pattern Recognition,* ***61***, pp. 650–662.

[27] Sarkar, S., Lore, K. G., Sarkar, S., Ramanan, V., Chakravarthy, S. R., Phoha, S., and Ray, A., 2015. "Early detection of combustion instability from hi-speed flame images via deep learning and symbolic time series analysis". In Annual Conf. of the Prognostics and Health Management.

[28] Sarkar, S., Lore, K. G., and Sarkar, S., 2015. "Early detec-

tion of combustion instability by neural-symbolic analysis on hi-speed video". In Proceedings of the 2015th International Conference on Cognitive Computation: Integrating Neural and Symbolic Approaches-Volume 1583, CEUR-WS. org, pp. 93–101.

[29] Akintayo, A., Lore, K. G., Sarkar, S., and Sarkar, S., 2016. "Prognostics of combustion instabilities from hi-speed flame video using a deep convolutional selective autoencoder". *International Journal of Prognostics and Health Management,* ***7***(023), pp. 1–14.

[30] Ghosal, S., Akintayo, A., Boor, P., and Sarkar, S. "High speed video-based health monitoring using 3d deep learning".

[31] Heckl, M. A., 1988. "Active control of the noise from a rijke tube". *Journal of Sound and Vibration,* ***124***(1), pp. 117–133.

[32] Ray, A., 2004. "Symbolic dynamic analysis of complex systems for anomaly detection". *Signal Processing,* ***84***(7), pp. 1115–1130.

[33] LeCun, Y., Bengio, Y., et al., 1995. "Convolutional networks for images, speech, and time series". *The handbook of brain theory and neural networks,* ***3361***(10), p. 1995.

[34] Simonyan, K., and Zisserman, A., 2014. "Very deep convolutional networks for large-scale image recognition". *arXiv preprint arXiv:1409.1556*.

[35] Ioffe, S., and Szegedy, C., 2015. "Batch normalization: Accelerating deep network training by reducing internal covariate shift". *arXiv preprint arXiv:1502.03167*.

[36] Hinton, G. E., Srivastava, N., Krizhevsky, A., Sutskever, I., and Salakhutdinov, R. R., 2012. "Improving neural networks by preventing co-adaptation of feature detectors". *arXiv preprint arXiv:1207.0580*.

[37] Chollet, F., et al., 2015. Keras.

[38] Abadi, M., Barham, P., Chen, J., Chen, Z., Davis, A., Dean, J., Devin, M., Ghemawat, S., Irving, G., Isard, M., et al., 2016. "Tensorflow: A system for large-scale machine learning.". In OSDI, Vol. 16, pp. 265–283.

[39] Kingma, D. P., and Ba, J., 2014. "Adam: A method for stochastic optimization". *arXiv preprint arXiv:1412.6980*.

[40] Pedregosa, F., Varoquaux, G., Gramfort, A., Michel, V., Thirion, B., Grisel, O., Blondel, M., Prettenhofer, P., Weiss, R., Dubourg, V., Vanderplas, J., Passos, A., Cournapeau, D., Brucher, M., Perrot, M., and Duchesnay, E., 2011. "Scikit-learn: Machine learning in Python". *Journal of Machine Learning Research,* ***12***, pp. 2825–2830.